Life-cycle exergetic efficiency and CO2 intensity of diabatic and adiabatic compressed air energy storage systems

Baghirov, Boyukagha; Hoornahad, Sahar; Voskov, Denis; Farajzadeh, Rouhi

DOI
10.1016/j.est.2025.118572

Publication date
2025

Document Version
Final published version

Published in
Journal of Energy Storage

Journal of Energy Storage 139 (2025) 118572

Contents lists available at ScienceDirect

Journal of Energy Storage

journal homepage: www.elsevier.com/locate/est

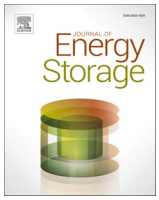

Research papers

Life-cycle exergetic efficiency and CO_2 intensity of diabatic and adiabatic compressed air energy storage systems

Boyukagha Baghirov [a,*], Sahar Hoornahad [b], Denis Voskov [a,c], Rouhi Farajzadeh [a,b]

[a] Department of Geoscience and Engineering, Delft University of Technology, the Netherlands
[b] Shell Global Solutions International, the Netherlands
[c] Department of Energy Science and Engineering, Stanford University, USA

A B S T R A C T

This study uses the concept of exergy-return on exergy-investment (ERoEI) to evaluate the life-cycle exergetic efficiency and CO_2 intensity (grams CO_2 per MJ of electricity) of (diabatic and adiabatic) compressed air energy storage (CAES) systems. Several CAES configurations are assessed under defined system boundaries, including diabatic systems powered by methane (CH_4) or hydrogen (H_2), and adiabatic system with a thermal energy storage (TES) facility.

The results show that conventional (diabatic) CAES system powered by natural gas has the lower exergetic efficiency and higher CO_2 intensity compared to adiabatic CAES due to the heat dissipation during compression stage and additional fuel requirements for reheating the air during expansion. Integrating carbon capture and storage (CCS) plant with conventional diabatic CAES can nearly halve the CO_2 intensity for electricity generation although the additional exergy investment for the CCS process reduces the exergetic efficiency of the system. Transitioning to green H_2 (produced from low-carbon electricity) as the primary turbine fuel in the diabatic CAES results in a 65–76 % reduction in CO_2 intensity. However, the average exergetic efficiency of system decreases by around 10 %, mainly due to the substantial exergy investment associated with hydrogen production. It is also found that the adiabatic CAES system integrated with TES demonstrates the highest thermodynamic and environmental performance. When 100 % of compression heat is captured and reused during discharge phase, the system reaches ERoEI values up to 61 % with CO_2 intensity of 12–26 g CO_2 per MJe.

Disclaimer: The results and performance metrics presented in this study are based on modelled scenarios and literature-derived parameters under defined system boundaries. Actual performance of CAES systems may vary depending on site-specific conditions, technology maturity, and operational configurations. All efficiency values, CO_2 intensity estimates, and comparative assessments should be interpreted within the context of the assumptions and limitations described herein. This study does not constitute a commercial endorsement or performance guarantee. The authors have made every effort to ensure accuracy but accept no liability for decisions made based on this analysis.

Nomenclature

Ex	Exergy (MJ)
$\dot{ex}$	Exergy rate (MJ/s)
ERoEI	Exergy Return on Exergy Investment
T	Temperature (K)
h	Specific enthalpy (kJ/kg)
s	Specific entropy (kJ/kg K)
$\dot{m}$	Mass rate (kg/s)
m	Mass (kg)
c	Specific heat capacity (kJ/ K)
CO_2	CO_2 Intensity (g-CO_2/MJe)
L	Leak rate
W	Specific carbon emission (g-CO_2/MJ)
G	Global Warming Potential Value

Subscripts

out	Outlet
in	Inlet
0	Environment state
comp	Compressor
exp	Expansion
t	Turbine
m	Motor
g	Generator
b	Burner
mech	Mechanical
ccs	Carbon capture storage
tes	Thermal energy storage
h	Heat
f	Fuel
ch	Chemical
pr	Production
eq.int	Equivalent intensity
leak	Leakage
dir	Direct
indir	Indirect

Greek symbols

η – efficiency

(continued on next column)

(continued)

1. Introduction

Over the past years, the extensive use of fossil fuels has led to significant environmental issues primarily due to the release of greenhouse gases. To decrease reliance on fossil fuels, there has been a substantial increase in the use of renewable energy sources [1]. According to the International Energy Agency (IEA), global renewable energy production is growing at an average annual rate of 1.1 %, accounting for approximately 30 % of the total electricity generation in 2023 [2]. However, the intermittent nature of renewable energy sources like wind and solar

* Corresponding author.
E-mail address: b.baghirov@tudelft.nl (B. Baghirov).

https://doi.org/10.1016/j.est.2025.118572
Received 20 March 2025; Received in revised form 20 July 2025; Accepted 24 September 2025
Available online 10 October 2025

makes it challenging to provide a continuous electricity supply [3]. Electrical energy storage (EES) technologies offer a promising solution to address this problem. By storing excess electricity during times of low demand and releasing it in high demand period, EES systems can stabilize the power balance over time [3,4]. Different EES technologies have been investigated in the literature. The examples include Pumped Hydro Storage (PHS), Compressed Air Energy Storage (CAES), batteries, fuel cells, flywheels. The PHS and CAES systems can supply large grid-scale (>100 MW) electricity. Nevertheless, the implementation of PHS faces challenges due to geographical limitations, such as availability of suitable sites and water resources, and ecological concerns regarding the potential habitat destruction caused by dam construction [4–7].

Compressed Air Energy Storage (CAES) is a promising technology for storing large grid-scale (>100 MW) electricity [4,8–10]. CAES systems operate by compressing air during periods of low electricity demand and storing it in underground geological formations. This technology usually utilizes salt caverns or depleted gas fields due to their capacity for storing large amounts of energy. During periods of high electricity demand, the compressed air is released, heated, and expanded through a turbine to generate electricity [4,8–10]. CAES systems offer several benefits, including low operating costs, stable operation, and quick start-up capabilities. These advantages enhance the feasibility and scalability of CAES, especially in regions with favorable geological conditions [4,8–10]. Currently, there are two CAES plants in Germany and USA that have been producing electricity for decades with capacity of 321 MW and 110 MW, respectively [4,8].

CAES systems can be classified into diabatic and adiabatic types based on their management of thermal energy in compression phase [4,8,9]. Diabatic CAES (D-CAES) systems release the generated heat during compression to the environment, which requires additional fuel to reheat the air during the expansion stage. This defines thermodynamic cycle where air is compressed and cooled, stored under high pressure, then externally reheated before expansion to generate electricity. Reheating is typically achieved by combusting fuels such as methane (CH_4), hydrogen (H_2), biogas, or their blends. While D-CAES systems are technically simpler and have lower initial capital costs compared to adiabatic systems, it is characterized by low overall efficiency and large carbon dioxide (CO_2) emissions due to use of fossil fuels and dissipating heat [4,8,9]. To address these issues, the concept of Adiabatic CAES (A-CAES) has been proposed. Unlike D-CAES, A-CAES systems capture and store thermal energy during compression and utilize it to reheat the air during the expansion phase. The captured heat can be stored in thermal energy facilities, such as molten salts, natural rocks, packed beds and liquid tanks. Then, the stored heat can then be utilized with the help of heat exchangers to meet the required heat demand during the discharging phase for expanding the air. This internal heat integration forms a close adiabatic thermodynamic cycle and minimizing external heat exchange in the system. As a result, A-CAES systems, enhance the overall efficiency and reduce carbon emission of the process. Nevertheless, a major challenge of A-CAES systems is to identify the suitable thermal storage media to efficiently capture heat and store it for a long period without heat loss [8–11].

Currently, three main techniques are used as thermal storage options in the A-CAES applications: sensible, latent and thermochemical heat storage, among which the sensible heat storage is the most widely used and mature method. It stores heat by changing temperature of system without a phase change. The liquid media, such as water or oil tanks or packed beds with solid media like sand or rocks are used in this method. In addition, the large heat exchange area in packed-bed configurations helps minimize heat loss [10,12–14]. The latent heat storage method provides higher energy storage density because the heat is stored by changing the phase of the applied media, such as molten salt, paraffin wax, and water/ice. Both sensible and latent heat storage methods can operate at temperature up to 1000 °C, depending on the used materials [10,12–14]. In the thermochemical method the heat is stored in the chemical bonds of the generated substance via reversible chemical reactions. Common thermochemical reactions include metal redox reactions with oxygen exchange, carbonate decomposition and reformation, and reversible metal hydrate formation. The thermochemical systems could keep temperatures as high as 1200 °C. However, the reaction efficiency decreases over the time. Furthermore, compared to sensible and latent heat storage methods, this method is less mature and more research is required to develop it further [12,13,15].

Recent literatures [9,11,16–24], have explored various configurations and optimization scenarios to improve the overall efficiency of both diabatic and adiabatic CAES systems. Thermodynamic analysis, particularly using the concept of exergy, is a commonly used method to evaluate the sustainability (measured by exergetic efficiency) of the considered systems and to identify potential energy losses and weak points within the system [9,16,25,26]. Kim et al. [9] performed an exergy analysis of the A-CAES system with thermal storage option and calculated 68 % efficiency when storing released heat of compression in TES. Barbour et al. [11] conducted an exergy analysis of the A-CAES system using packed beds as thermal storage media. Their results demonstrated that an exergy efficiency of up to 70 % is achievable, with the most exergy destruction occurring in the compressors and expanders. Szablowskiet et al. [16] found a round-trip efficiency of 50 % for the A-CAES system with oil tank, demonstrating the compressors and turbines as the main sources of exergy destruction. Wolf and Budt [17] conducted a study to integrate adiabatic CAES with TES, estimating an exergy efficiency of approximately 56 %. They showed that A-CAES with lower TES temperatures can be economically more viable due to quicker start-up times. Furthermore, Pickard et al. [18] performed an integrated energy and exergy analysis of an advanced A-CAES system, estimating a cycle efficiency of roughly 50–64 %. Accordingly, it was noted that the exergy (heat) losses and inefficiencies of the motor, compressor, generator, and expanders impose limitations on achieving higher efficiency. Yu et al. [19] investigated a CAES system integrated with packed-bed latent thermal energy storage using phase change materials (PCMs). They tested different combinations based on the thermophysical properties (melting temperature, density, latent heat, specific heat capacity, thermal conductivity) of PCMs and found that round-trip efficiencies ranged from 43.4 % to 63.5 %. Chen et al. [20] proposed a novel integration of water-based carbon capture with an adiabatic CAES system, using flue gas with elevated CO_2 concentration as the working fluid. Their thermodynamic analysis shows that the integrated system attains an exergy efficiency of 69.6 %, while the water-based capture process consumes only 354 kWh/t CO_2, substantially less than conventional amine-based methods. Ding et al. [5] introduced a novel combined cooling, heating, and power (CCHP) system for D-CAES, which achieves an exergy efficiency of 51 %. However, they found that the combustion chamber as the main source of exergy destruction, responsible for more than half of the total exergy losses. Sciacovelli et al. [21] focused on dynamic performance of packed bed TES and found that A-CAES can achieve exergy efficiency from 60 % to 70 % when the TES system operates at thermal storage efficiencies exceeding 90–100 %. Elmegaarda and Brix [22] found that the overall efficiency of conventional CAES systems exhibit relatively low efficiencies ranging from 25 % to 45 %, with main exergy loss occurring in combustion and heat transfer processes during the discharge phase. However, adiabatic CAES presents a promising alternative, potentially reaching efficiencies as high as 70 %. Xue et al. [23] analysed a CAES system integrated with a water electrolysis unit and an H_2-fuelled gas turbine, reporting a CAES subsystem with exergy efficiency of 64.28 %. Safaei and Aziz [24] found that an A-CAES system utilizing physical heat storage achieved the highest exergy efficiency, with 69.5 %. In contrast, the analysed conventional D-CAES system attained 54.3 % efficiency, while the H_2-powered system demonstrated the lowest efficiency, at around 35 % due to significant exergy loss in the electrolyser.

In summary, although numerous studies have proposed various solutions to enhance the thermodynamic performance of Compressed Air Energy Storage (CAES) systems, there remains a substantial need for

further research to identify the most optimal configuration from both thermodynamic and environmental perspectives. To date, the literature has predominantly concentrated on thermodynamic (exergy) analysis, often neglecting the environmental impacts of these processes, particularly their carbon emissions. However, to comprehensively evaluate the sustainability of energy systems, it is imperative to integrate exergy efficiency assessments with evaluations of carbon dioxide (CO_2) intensity [27–29]. Furthermore, most existing exergy or energy analyses of CAES systems focus solely on the core operational phases (compression, storage, and expansion), while neglecting supporting processes such as fuel production and auxiliary energy use. This limited scope often leads to incomplete or overly optimistic assessments of system sustainability.

In this paper, we propose various scenarios for optimizing the performance of CAES systems and investigate them from both thermodynamic and environmental perspectives. In the first scenario, the integration of a Carbon Capture and Storage (CCS) plant within traditional D-CAES systems (powered by methane, CH_4) is examined, which can mitigate the CO_2 footprint of the process by capturing the CO_2 released from the combustion of CH_4 (D-CAES with CH_4 + CCS). The second scenario (D-CAES with hydrogen, H_2) involves the utilization of hydrogen as an alternative to methane in the traditional diabatic CAES systems (D-CAES with CH_4). Compared to other low-carbon fuels, such as ammonia (NH_3) or biofuels, higher (mass) energy density (118 MJ/kg), and clean-burning properties of H_2 offer the potential to enhance exergy efficiency and reduce carbon emissions. Another scenario explores an A-CAES system integrated with a TES facility (A-CAES with TES) to increase exergy efficiency and reduce CO_2 intensity by recovering compression heat and eliminating the need for fuel use. By comparing traditional diabatic systems with the proposed alternative configurations, we aim to identify the advantages and limitations of each approach.

The primary objective of this work is to bridge the gap between thermodynamic and environmental analyses by applying the concept of Exergy Returned on Exergy Invested (ERoEI) to the proposed CAES scenarios. ERoEI is a common method for examining the sustainability of energy systems from a thermodynamic perspective. ERoEI, or exergetic efficiency, represents the fraction of invested exergy that is converted into useful work. While conventional indicators such as round-trip efficiency (RTE) or energy efficiency are widely used in thermodynamic analysis, they typically overlook the quality of energy transformations and do not account for irreversible losses. In contrast, the exergy-based ERoEI metric provides a more rigorous sustainability indicator by incorporating both the quality and quantity of energy flows, based on the second law of thermodynamics. Building upon the ERoEI framework, the study further incorporates an environmental assessment through the calculation of operational CO_2 intensity, expressed in mass (grams) of CO_2 emitted per MJ of electricity generated. This integrated approach allows simultaneous evaluation of system performance from both thermodynamic and environmental perspectives [29–31].

Unlike previous studies, the proposed holistic framework adopts a life-cycle approach, which accounts for exergy investment at all stages of the entire process, from inception to operational end. This approach enables us to identify the scale and origin of thermodynamic inefficiencies at different stages of the life-cycle process and subsequently convert these inefficiencies into CO_2 equivalent intensity to accurately reflect the environmental impact of each segment [29–32].

In summary, based on ERoEI framework, the main contributions of this study are as follows:

- Development of a life-cycle-based ERoEI methodology for assessing thermodynamic and environmental performance of various CAES systems (diabatic and adiabatic).
- Introduction of a dual-indicator framework combining exergetic efficiency (ERoEI) with CO_2-equivalent intensity to holistically evaluate different CAES scenarios, including diabatic systems with CH_4 and H_2 (with and without CCS), and adiabatic CAES with TES.
- Integration of upstream auxiliary processes such as fuel (CH_4 or H_2) production and CCS energy penalties into the exergy and emission accounting.
- Identification and quantification of key sources of exergy loss and CO_2 emissions across the full CAES life-cycle.

The structure of this paper is as follows: First, we define the system boundaries for both diabatic and adiabatic CAES systems with describing their work principle. Based on these boundaries, we establish an exergy workflow, including work and material streams, to calculate exergy efficiency and CO_2 intensity for each system, including D-CAES with CH_4, D-CAES with CH_4 + CCS, D-CAES with H_2, A-CAES with TES. Next, we present our results in a comparative manner to identify the most optimal CAES scenario. The paper concludes with insightful remarks summarizing the findings.

2. System definition

Compressed Air Energy Storage (CAES) systems operate through two primary stages: charging and discharging (Fig. 1). During the charging phase, air is compressed using surplus electricity from low-carbon wind sources, thereby converting electrical energy into mechanical and thermal energy. The compressed air is subsequently stored in underground salt caverns. During the discharging phase, when electricity demand is elevated, the pressurized air is heated and expanded through a turbine to generate electricity. In this study, we examine two principal configurations of CAES systems: diabatic and adiabatic. Detailed descriptions of the configurations of these systems are provided in the subsequent sections. The inlet and outlet temperature and pressure values in the configurations (Fig. 2 and Fig. 3) were taken from published data [5,7–9,16,24,25,33–41].

2.1. Diabatic CAES

As mentioned previously, in the diabatic CAES system, the heat generated during the compression process is not recovered, necessitating the combustion of fuel during the discharging process. Fig. 2 illustrates the schematic of the diabatic CAES system, including the main process components and thermodynamic boundary conditions. During the charging stage, air is compressed up to 70 bar in two stages with a low-pressure (LP) and high-pressure (HP) compressors, increasing the compressor temperature up to 631 °C. Following the charging or compression process, the air is stored in a salt cavern, where the temperature and pressure are maintained at 20 °C and 70 bar, respectively. During periods of high electricity demand, the compressed air is released from the cavern and reheated in a combustor before entering the turbine. The reheating process can raise the air temperature as high as 825 °C and even up to 1650 °C, depending on the fuel type (CH_4 or H_2) [5,7,39,40].

When CH_4 is used, the inlet air temperature range can be from 825 °C to 1350 °C [5,7–9,25,35,39,40]. However, considering the higher energy density of H_2, the inlet temperature range increases to 1200 °C - 1650 °C [38]. In addition to higher temperature, which makes the discharging process more efficient, burning H_2 produces only water vapor, eliminating CO_2 emissions. However, the higher energy and economic cost of hydrogen production presents a significant challenge. Furthermore, while higher inlet temperatures can increase turbine output, they also pose difficulties in terms of finding materials that can resist such high temperatures [38].

During the discharging stage, the air expands through two turbines (low pressure and high pressure). After the first stage of the expansion, the air pressure decreases to 12.8 bar, with final outlet temperatures ranging between 468 °C and 876 °C. If CH_4 is used as the fuel, CO_2 is generated as a byproduct. Consequently, to mitigate these emissions, a CO_2 capture unit should be integrated into the process, which results in additional energy penalty. The pressure and temperature conditions of

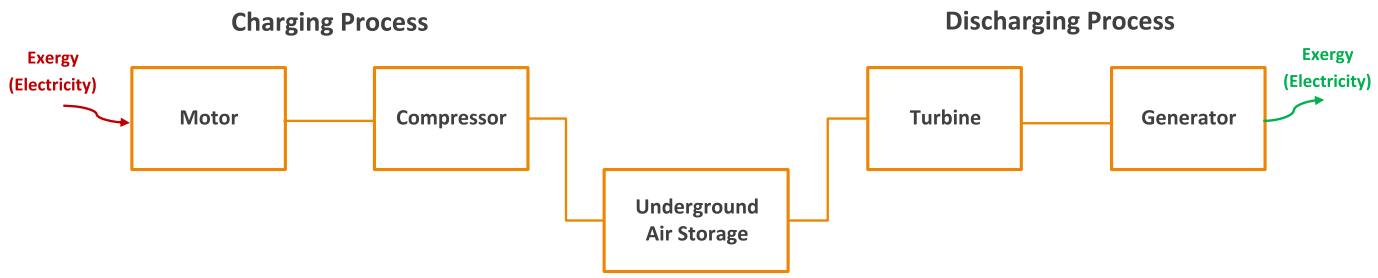

Fig. 1. Schematic view of a general CAES system using exergy concept.

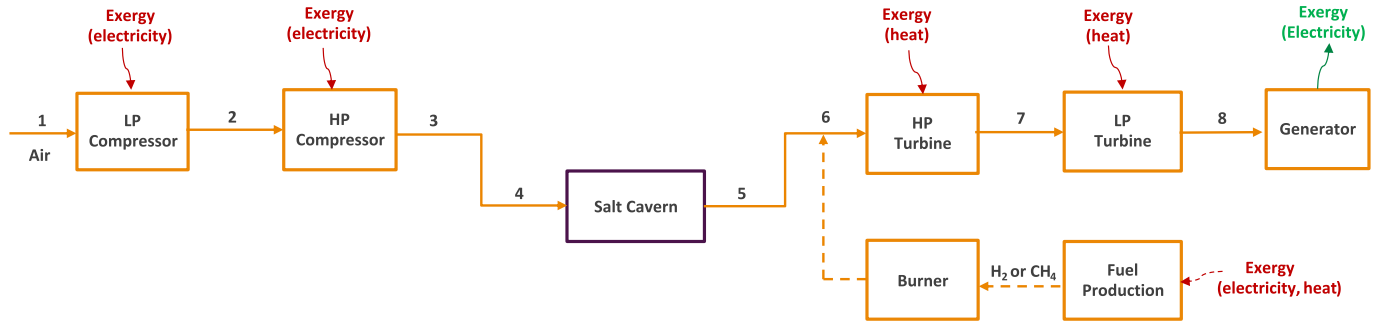

Fig. 2. Schematic view of the diabatic CAES system. Streams 1–8 represent the main air flow path, shown with solid lines. The dashed lines indicate the auxiliary fuel loop, which supplies heat to the turbine via fuel combustion.

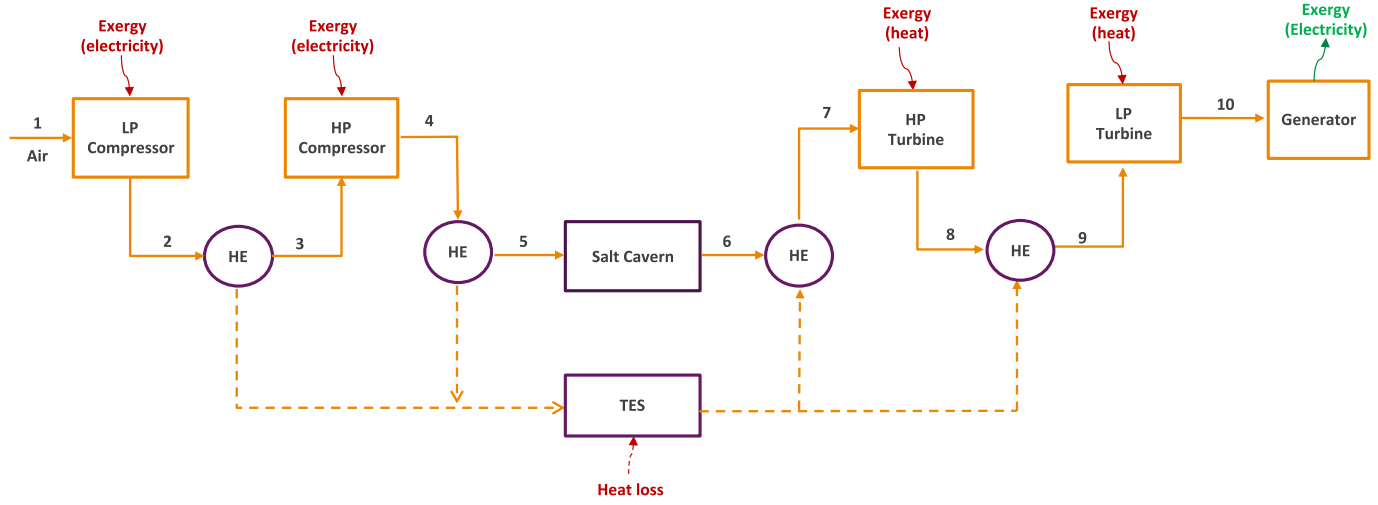

Fig. 3. Schematic view of the adiabatic CAES system. Streams 1–10 represent the main air flow path, shown with solid lines. The dashed lines indicate the auxiliary thermal energy storage loop, where compression heat is captured, stored, and reused during the expansion process.

each stream in the diabatic CAES system are summarized in Table 1.

2.2. Adiabatic CAES with thermal energy storage

The adiabatic CAES system, captures and stores the heat generated during compression in a Thermal Energy Storage (TES) facility, which is later used during the expansion phase. By storing the heat, the adiabatic system eliminates the usage of additional fuel and ensures a CO_2-neutral process [8–11].

The schematic view and system boundaries of the adiabatic CAES configuration are illustrated in Fig. 3. Similar to the conventional diabatic CAES systems, the process starts with compressing air to 70 bar in two stages, which increases the outlet air temperature to approximately 631 °C. Following each compression stage, the hot air passes through a heat exchanger (HE) and enters the packed bed (TES facility). Here, heat is exchanged with the gravel within the TES, which acts as a storage material, capturing heat for later use. Afterwards, the air enters the cavern at a nearly ambient temperature and high pressure (70 bar).

During the discharge process, energy is extracted by withdrawing high-pressure air from the cavern. The compressed air is initially heated using thermal energy stored in the TES, reaching a temperature of 630 °C prior to expansion. The air is then expanded through a two-stage turbine to generate electricity. The outlet temperature and pressure of the air are fixed at 134 °C and 1 bar, respectively, after the final turbine stage (Fig. 3) [42]. The pressure and temperature conditions of each stream are summarized in Table 2.

3. Life-cycle exergy analysis

Exergy analysis is robust thermodynamic that evaluate the quality

Table 1
Thermodynamic boundary conditions of air in each process stream shown in Fig. 2.

Stream No.	Temperature (°C)	Pressure (bar)	Description
1	20	1.01	Inlet of LP compressor
2	200	8.5	Outlet of LP compressor / Inlet of HP compressor
3	631	70	Outlet of HP compressor
4	20	70	Inlet of salt cavern (after cooling)
5	20	70	Outlet of salt cavern
6	825–1650	70	Inlet of HP turbine (after combustion heating)
7	550–950	12.8	Outlet of HP turbine / Inlet of LP turbine
8	468–876	1.01	Outlet of LP turbine

Table 2
Thermodynamic boundary conditions of air in each process stream shown in Fig. 3.

Stream No.	Temperature (°C)	Pressure (bar)	Description
1	20	1.01	Inlet of LP compressor
2	300	8.5	Outlet of LP compressor
3	200	8.5	Inlet of HP compressor
4	631	70	Outlet of HP compressor
5	20	70	Inlet of salt cavern (after heat transfer)
6	20	70	Outlet of salt cavern
7	630	70	Inlet of HP turbine (after reheating via TES)
8	300	11	Outlet of HP turbine
9	382	11	Inlet of LP turbine (after reheating via TES)
10	134	1.01	Outlet of LP turbine

and usefulness of energy within a system based on the second law of thermodynamics. In essence, exergy represents the maximum useful work that can be obtained from the system, when it moves into equilibrium with its environment. Unlike energy, exergy can be destroyed by irreversibility in system components, thereby revealing the true potential of an energy system. Assuming negligible potential, kinetic, and chemical effects, the exergy (MJ) of an air stream is given by [8,41,43]:

$$Ex = m \times ((h - h_0) - T_0(s - s_0)) \quad (1)$$

where h (kJ/kg) and s (kJ/kg K) are specific enthalpy and entropy, and subscript 0 denotes environmental conditions or dead state ($T_0 = 293$ K, $P_0 = 1$ bar).

In practice, especially for continuous flows, it is more useful to use exergy rate (MJ/s) in the analysis, where ṁ (kg/s) is mass flow rate of air.

$$\dot{ex} = \dot{m} \times ((h - h_0) - T_0(s - s_0)) \quad (2)$$

3.1. Exergy return on exergy investment (ERoEI)

Exergy Return on Exergy Investment (ERoEI) is an analytical metric for evaluating the thermodynamic and environmental performance of various energy systems. Here, we extend the application to examine the exergetic efficiency and CO_2 intensity of proposed diabatic and adiabatic CAES systems. Conventionally, ERoEI is defined as the ratio of exergy output (returned exergy rate) to exergy input (invested exergy rate) [29–31]:

$$EROEI = \frac{\dot{ex}_{returned}}{\dot{ex}_{invested}} \quad (3)$$

where $\dot{ex}_{returned}$ is the amount of the rate of gained exergy from the system and $\dot{ex}_{invested}$ is the total invested exergy rate in different stages of the process. Theoretically, the value of ERoEI can range from 0 to $+\infty$ [29,30].

The exergy analysis workflow is performed by splitting system into material ($\dot{ex}_{returned}$) and work ($\dot{ex}_{invested}$) streams depicted in Fig. 1. The workflow of exergy analysis has performed in Excell based Coolprop freeware. CoolProp uses Peng-Robinson and Soave-Redlich-Kwong (SRK) equation of state (standard cubic equation of state) for calculation of thermodynamic properties [44].

The main assumptions of the analysis are as follows:

- The system operates under steady state condition, with equal durations allocated for both the charging and discharging phases.
- The mass flow rate of air is maintained at a constant 120 kg/s during both charging and discharging phases.
- Air leakage is considered negligible throughout the process.
- In the D-CAES configuration, either H_2 or CH_4 is used as a fuel, with respective chemical exergy values of 118 MJ/kg and 51.8 MJ/kg [45].
- In the A-CAES configuration, the exergy requirement for heat exchangers is considered negligible.

3.1.1. Work stream

In this section, we introduce the work stream of both D-CAES and A-CAES systems. The work stream is the total exergy investment during the charging and discharging phases, including air compression, injection, and withdrawal. Furthermore, all fuel consumption and exergy investments associated with fuel generation are included in this analysis. Specific references to either the diabatic or adiabatic system are indicated in brackets where applicable.

3.1.1.1. Compression. Initially, air is compressed from atmospheric pressure to 70 bar through both low- and high-pressure compression stages. In the diabatic CAES (D-CAES) system, the heat generated from compression is released into the atmosphere, whereas in the adiabatic CAES (A-CAES) system, this heat is captured and recovered. The exergy consumption rate of the compression process is calculated using Eq. 4 referred to as the theoretical exergy of compression [9,41,46].

$$\dot{ex}_{comp} = \dot{m}_{air} \times ((h_{out} - h_{in}) - T_0(s_{out} - s_{in})) \quad (4)$$

where h_{out} (kJ/kg), h_{in} (kJ/kg) are the specific enthalpies of the output and input streams at a given pressure and temperature; s_{out} (kJ/kg K), s_{in} (kJ/kg K) are the specific entropies of the output and input streams at a given pressure and temperature, $\dot{m}_{air}$ is the mass flow rate of air (kg/s), and T_0 is the ambient temperature, 293 K.

To obtain the practical exergy rate, the efficiencies of the compressor and motor are considered (Table 3). Thus,

Table 3
Main assumptions and parameters for performing life-cycle exergy analysis.

Parameter	Value	Reference
$\dot{m}$	120 kg/s	–
c_{air}	1.01 kJ/K	[11]
η_c	70–90 %	[51,52]
η_b	80–90 %	[25,53]
η_t	70–93 %	[5,54]
η_m	90–98 %	[23,55,56]
η_g	90–98 %	[23,55,56]
$\eta_{mech.}$	100 %	[5]
η_{tes}	90–100 %	[21,46]
η_{ccs}	80–90 %	[50]
$Ex_{pr.}$ *(blue H_2)*	165–296 MJ/kg H_2	[48,49,57]
$Ex_{pr.}$ *(green H_2)*	169–252 MJ/kg H_2	[49,58,59]
$Ex_{pr.}$ *(CH_4)*	3–8 MJ/kg CH_4	[30]

$$\dot{ex}_{comp} = \frac{\dot{m}_{air} \times ((h_{out} - h_{in}) - T_0(s_{out} - s_{in}))}{\eta_c \times \eta_m} \quad (5)$$

3.1.1.2. Heat demand for air expansion (D-CAES). In the diabatic CAES configuration, the heat generated during the charging process remains unrecovered. Consequently, fuel combustion is required during the discharging process to expand air and drive the turbine for electricity generation. Depending on the selected fuel (CH_4 or H_2), turbine inlet temperatures can range from 850 °C to 1650 °C. The theoretical exergy rate of the heat demand can be estimated using Eq. 6 [11,43,46,47].

$$\dot{ex}_h = \frac{c_{air} \times \dot{m}_{air} \times \left(T_{in} - T_{out} - T_0 ln \frac{T_{in}}{T_{out}}\right)}{\eta_b} \quad (6)$$

where c_{air} (kJ/K) is specific heat capacity of air, T_{in} (K) is the air temperature of the air in the inlet of the turbine, T_{out} (K) is the air temperature in the cavern outlet, and η_b is the burner efficiency.

3.1.1.3. Production of consumed fuel (D-CAES). After estimating the heat demand for air expansion during the discharging phase, the mass rate of consumed fuel (kg/s) is calculated using the following equation:

$$\dot{m}_f = \frac{\dot{ex}_{h.}}{Ex_{ch.}} \quad (7)$$

where, $Ex_{ch.}$ is the fuel chemical exergy. The exergy rate for producing the fuel (Ex_f) is determined using Eq. 8.

$$\dot{ex}_f = \dot{m}_f \times Ex_{pr.} \quad (8)$$

Here, $Ex_{pr.}$ is the exergy required to produce 1 kg H_2 or CH_4, which varies depending on the selected production method. In the analysis, hydrogen is considered to produce from two sources: blue H_2, produced from natural gas with the capture of CO_2 generated during the process, and green H_2, produced through water electrolysis process powered by renewable low-carbon energy (wind or solar) source (Table 3) [48,49].

3.1.1.4. Carbon capture and storage (D-CAES). The exergy requirement for CO_2 capture and storage $\left(\dot{ex}_{ccs}\right)$ is assumed to be between 2.5 and 6 MJ/kg CO_2, using a monoethanolamine (MEA) based method, with a capture efficiency of 80–90 % [29,30,50].

3.1.2. Material stream

The material stream of the D-CAES and A-CAES systems refers to the amount of useful work obtained from the turbine during the discharging process, which is converted into electricity.

3.1.2.1. Air expansion. This returned exergy results from the expansion of compressed air, which drives the turbine to produce electricity. In the A-CAES system, the required heat for air expansion is supplied from a thermal energy storage (TES) facility, whereas in the D-CAES system, it is obtained through fuel combustion. The final exergy output of the turbine depends on the inlet and outlet temperatures and air pressure. For an isentropic expansion process the exergy rate is estimated from [21,41,46]:

$$\dot{ex}_{exp.} = \dot{m}_{air} \times (h_{in} - h_{out}) \quad (9)$$

The practical exergy rate is calculated by considering efficiency of turbine, generator and TES facility (Table 3):

$$\dot{ex}_{exp.} = \dot{m}_{air} \times (h_{in} - h_{out}) \times \eta_t \times \eta_g \times \eta_{tes} \quad (10)$$

3.1.2.2. Thermal energy storage (TES) facility (A-CAES). In this study, a sensible heat storage method - packed gravel bed is assumed to use as a TES facility to store the heat captured during the compression stage. We assume the efficiency of the thermal storage facility to be between 90 % and 100 % [21,46], corresponding to 10 % to 0 % heat loss.

3.2. CO_2 equivalent intensity

After estimating the invested exergy rates, the total CO_2 equivalent intensity of the process can be calculated. CO_2 intensity is defined as the mass of CO_2 released per unit of exergy (grams of CO_2 per megajoule electricity, g-CO_2/MJe) [29,30]. Therefore, it is essential to first estimate the mass rate of CO_2 emitted over the entire life cycle of the process. To better evaluate the sources of emissions, they are classified into two categories: direct emissions and indirect emissions. Direct emissions refer to those generated directly during the active operations of the CAES system, such as air compression and fuel combustion. The indirect emissions arise from life-cyclic activities that support the operation but occur outside of the immediate processes such as fuel production and leakage. The total CO_2 emission is the sum of direct and indirect emissions. Final CO_2 intensity of the process can be expressed as:

$$CO_{2eq.int} = \frac{\dot{m}^{co2}_{dir.} + \dot{m}^{co2}_{indir.}}{\dot{ex}_{returned}} \quad (11)$$

To calculate the CO_2 intensity separately for diabatic and adiabat CAES systems, the following assumptions are made:

- This study considers only CO_{2eq} emissions generate in the operational phase of system. Emissions related to infrastructure, construction, material production, and decommissioning are excluded from the analysis.
- The compression stage is powered by low-carbon electricity sources, assumed to be provided by offshore windmills, with a specific carbon intensity of 7 g-CO_{2eq}/MJe [60].
- The specific CO_2 intensity of CH_4 combustion is 55 g-CO_2/MJ [61].
- The CO_2 intensity of H_2 production assumed to be 1–5 kg CO_2/kg H_2 for the blue H_2 (from natural gas with CCS) and 1–3 kg CO_2/kg H_2 for the green H_2 (from electrolysis using wind or solar energy) [49,57,62].
- Leakage rates during fuel production stage are assumed to be 1–1.5 % for blue H_2, 2–4 % for green H_2 and 0–1.5 % for CH_4 [29,63].
- The global warming potential (GWP) values for CH_4 and H_2 over a 100-year periods are 28 and 12, respectively [64,65].

In D-CAES system, the total equivalent mass (rate) of generated CO_2 is the sum of emissions from compression $\left(\dot{m}^{co2}_{comp.}\right)$, fuel combustion $\left(\dot{m}^{co2}_{h.}\right)$, and fuel production $\left(\dot{m}^{co2}_{f.}\right)$ stages. Furthermore, CH_4 and H_2 leakages $\left(\dot{m}^{co2}_{leak.}\right)$ during the fuel production stage are included in the analysis, with adjustments made based on their global warming potential (GWP) over a 100-year period:

$$CO_{2eq.int} = \frac{\dot{m}^{co2}_{comp.} + \dot{m}^{co2}_{h.} + \dot{m}^{co2}_{f.} + \dot{m}^{co2}_{leak.}}{\dot{ex}_{returned}} \quad (12)$$

In more detail, in the formula, CO_2 emissions from compression $\left(\dot{m}^{co2}_{comp.}\right)$, and heat $\left(\dot{m}^{co2}_{h.}\right)$ generation from fuel combustion are determined by multiplying the exergy investment rate for these processes by the specific CO_2 emissions associated with each energy source. The emissions from the fuel production stage $\left(\dot{m}^{co2}_{f.}\right)$ are estimated by adjusting the specific CO_2 intensity values of the selected fuel production method. The method to calculate CO_2 equivalent emissions from leakage stage $\left(\dot{m}^{co2}_{leak.}\right)$ accounts for the leak rate and the GWP values of specific gases (CH_4 or H_2) as described in our previous work

[29]. For the A-CAES system, the equation can be expressed as,

$$CO_{2eq,int} = \frac{\dot{m}^{co2}_{comp.}}{\dot{ex}_{returned}} \quad (13)$$

4. Results and discussions

This section presents the outcomes of a life-cycle exergy analysis conducted on five distinct Compressed Air Energy Storage (CAES) scenarios, which are primarily differentiated by their heat management and fuel consumption strategies. Initially, the exergetic efficiency and principal exergy losses of each system are scrutinized. Subsequently, the CO_2 equivalent intensity of the proposed CAES systems is analysed in a comparative context. Finally, the results are compared with findings from related literature. The entire exergy analysis workflow was executed utilizing an Excel-based platform, which is integrated with the CoolProp freeware library.

4.1. Exergetic efficiency (ERoEI)

The exergy analysis starts with the calculation of exergy rates for each process step within the work and material streams, as depicted in Fig. 2 and Fig. 3. The calculated ranges of invested and returned exergy rates are presented in Table 4 for both diabatic and adiabatic CAES configurations. These values are derived using the equations (Eqs. 4–10) outlined in the previous section.

Fig. 4 illustrates the maximum and minimum estimated ERoEI values of each scenario. It is important to mention that in addition to maximum and minimum ranges of ERoEI, in each scenario the invested exergy rates should correspond to correct output rate. For example, in the diabatic CAES systems, the maximum ERoEI is associated with the lower exergy consumption in the compressor stage coupled with the higher turbine output, while the minimum ERoEI corresponds to higher compressor energy demand, lower turbine output, and consequently reduced fuel consumption. A detailed example of the calculation is given below for the D-CAES with CH_4 configuration:

$$ERoEI\ (D-CAES\ with\ CH_4)_{max} = \frac{91.2}{97.2+126.3+8.8} = 0.39$$

$$ERoEI\ (D-CAES\ with\ CH_4)_{min} = \frac{32.4}{132+58.8+6.3} = 0.16$$

The same calculation procedure was used for the other proposed configurations. Overall, the results of analysis indicate that traditional D-CAES system powered by CH_4 exhibits low exergetic efficiency, in the range of 0.16–0.39, primarily due to significant heat dissipation during the charging phase. Adding an energy-intensive CCS plant to this system leads to additional exergy loss. The final exergetic efficiency for D-CAES with CH_4 and CCS (CH_4 + CCS) is calculated in the range of 0.15–0.36 (Fig. 4). This reveals that a substantial part of the exergy input (63–85 %) is lost at different stages of the system. Fig. 5 shows that the largest exergy loss for this scenario (34 %) occurs in the compression process.

Table 4
Main input parameters used to calculate exergy rates of the work and material streams for diabatic and adiabatic (with TES) CAES systems.

Invested and Returned Exergy Rates	Applicable Scenario	Value (MJ/s)
$\dot{ex}_{comp}$	D-CAES and A-CAES	97.2–132
$\dot{ex}_h$	D-CAES with CH_4	58.8–126.3
$\dot{ex}_h$	D-CAES with H_2	84.4–145.6
$\dot{ex}_f$	D-CAES with CH_4	6.3–8.8
$\dot{ex}_{ccs}$	D-CAES with CH_4 + CCS	17.3–19.5
$\dot{ex}_f$	D-CAES with blue H_2	216.2–241.5
$\dot{ex}_f$	D-CAES with green H_2	178.9–208.5
$\dot{ex}_{exp.}$	D-CAES with CH_4	32.4–91.2
$\dot{ex}_{exp.}$	D-CAES with H_2	48–103.2
$\dot{ex}_{exp.}$	A-CAES with TES	36–58.8

The heat consumption for air expansion is second highest contributor accounting for 27 % loss. Integration of CCS plant and inefficiencies in turbine operation consume nearly equal portion, comprising 5–6 % of exergy input. Since CH_4 is a primary energy source, its production requires minimal exergy demand.

When using H_2 instead of CH_4 to power the turbine, the inlet temperate is higher due to higher lower heating value (LHV) of H_2. As previously discussed, the total electricity output from the turbine depends on inlet and outlet temperatures and pressures. Therefore, in these scenarios (D-CAES with blue and green H_2), the elevated inlet temperature results in greater power output (returned exergy). However, producing H_2 fuel requires substantial amount of energy (Table 4) and offsets this increased exergy gain (Fig. 4). As shown from Fig. 6, H_2 production constitutes a significant share of the total exergy investment compared to CH_4 production, resulting in a notable reduction in ERoEI. On average, the H_2-fuelled system exhibits approximately 10 % lower life-cycle exergetic efficiency than the CH_4-based diabatic system due to the energy intensive H_2 production stage. In the H_2 fuelled D-CAES system, compression and heat consumption are the second largest contributors, each comprising 21 % of the total exergy input.

The maximum ERoEI for the A-CAES with the TES reaches 61 % when heat recovery efficiency is 100 %, i.e., the case with no heat loss (Fig. 4). The higher efficiency is mainly due to the heat recovery during compression stage, which is used to heat up air in the expansion process. However, the ERoEI of this system is strongly dependent on the thermal efficiency of the storage facility. For example, with 90 % TES efficiency (10 % heat loss in TES), the maximum exergetic efficiency drops to 55 %. In the A-CAES system, the main exergy loss is in the compression stage, with 46 % of supplied exergy. With typical TES efficiencies ranging between 90 and 100 %, only a minor fraction (3 %) of the available exergy is destructed due to heat loss. Additionally, inefficiencies in the turbine account for around 7 % of the total exergy input. Consequently, the remaining 44 % of the exergy input is returned as useful output, representing the average life-cycle exergetic efficiency of this configuration.

In summary, among the analysed configurations, the A-CAES system with TES demonstrates the highest ERoEI, providing, on average, a 18 % and 27 % increase in thermodynamic efficiency compared to D-CAES systems fuelled by CH_4 and H_2, respectively. However, it is important to note that most industrial TES applications currently offer storage durations ranging from only a few hours to a few days with minimal or no heat loss. For longer durations, thermal loss becomes significant, leading to a reduction in exergetic efficiency. To address this limitation, future enhancements could focus directly on improving the storge capacity and duration of TES facility with combining sensible and latent heat storage options which can enhance system exergy efficiency. Alternatively, a hybrid configuration integrating diabatic and adiabatic CAES systems could also be considered to extend storage duration while benefiting the advantages of both approaches.

4.2. CO_2 equivalent intensity

Following the exergy analysis, the CO_2 intensity of the proposed configurations was estimated using Eqs. 12 and 13.

Fig. 7 presents the minimum and maximum life-cycle CO_2 equivalent intensity of the different CAES scenarios. As shown in Fig. 7, the D-CAES system exhibits the highest carbon footprint, primarily due to CO_2 emissions from CH_4 combustion during the discharging phase. Moreover, CH_4 leakage (0–1.5 %) can occur during fuel production and supply. CH_4 has 28 times more global warming potential (GWP) compared to CO_2 over a 100-year period [29,64]. However, integrating a CCS plant with a capture efficiency of 80–90 % significantly reduces emissions from the combustion stage, lowering the overall CO_2 intensity by an average of 50 %.

Another promising strategy to reduce the carbon emission of the D-CAES systems is to employ green H_2 as fuel during the discharge phase.

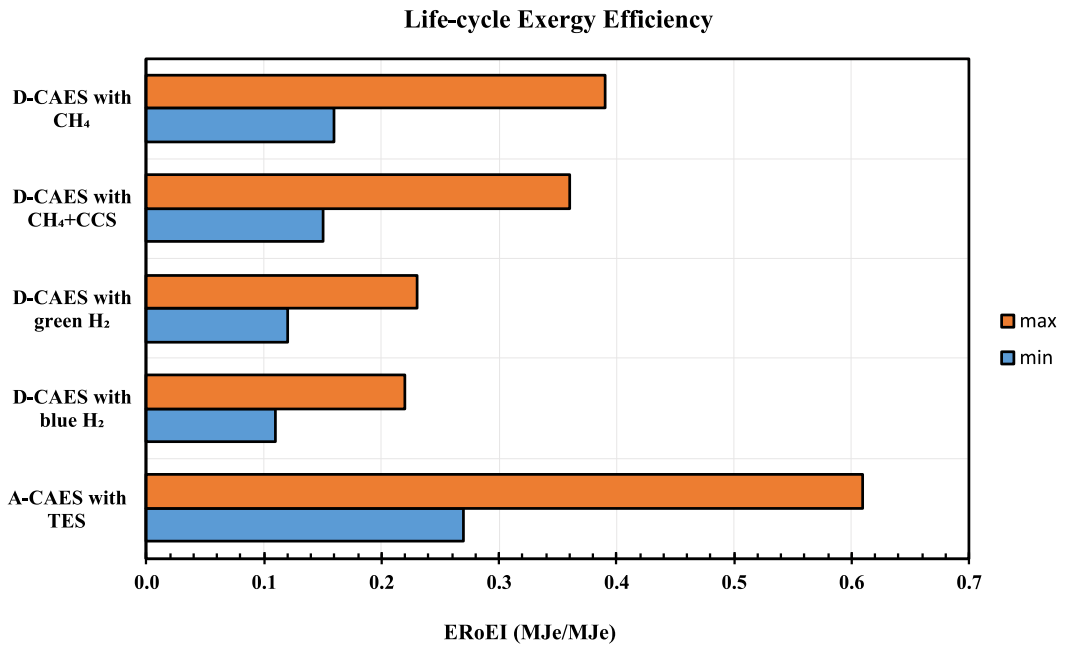

Fig. 4. Maximum and Minimum values of Exergy Return on Exergy Investment (ERoEI) or exergy efficiency of different CAES systems.

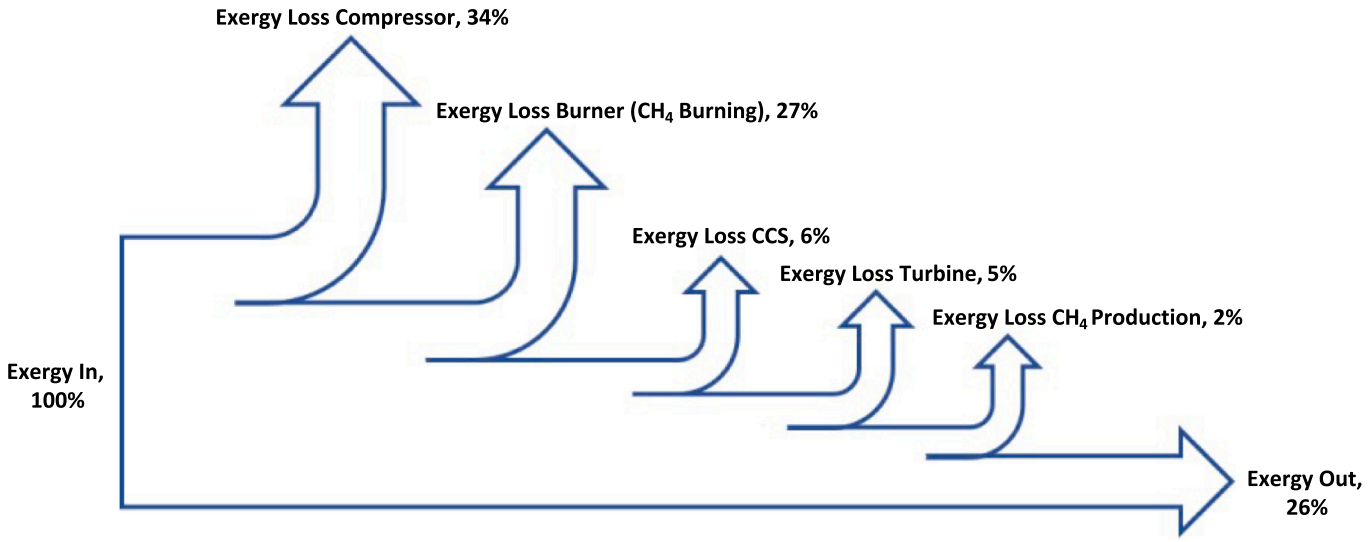

Fig. 5. Exergy flow distribution and average exergy loss fractions for diabatic CAES systems powered by CH_4 (with CCS option).

Although H_2 combustion itself does not emit CO_2, the production of green H_2, even when powered by low-carbon wind resources, generates approximately 1–3 kg CO_2 per kg of H_2 [59,62]. Additionally, 2–4 % of H_2 leakage may occur during the production and utilization, necessitating its inclusion in the calculations as equivalent intensity conversion [63]. The GWP of H_2 is 12 compared to CO_2 in 100 year period [65]. Nonetheless, the results remain optimistic, with only 21–70 g of CO_2 generated per MJ of electricity production, which is 65–76 % less than the conventional diabatic CAES scenario (Fig. 7). In contrast, utilization of blue H_2 instead of green H_2 does not lead to a significant reduction in CO_2 intensity. While integration of CCS plant in the H_2 production stage decreases carbon emission, the process still releases 1–5 kg CO_2 per kg of H_2 [49,62]. Additionally, during manufacturing of blue H_2, 1–1.5 % of H_2 leakage and 0–1.5 % of CH_4 leakage (during reforming, oxidation process) are assumed [29,63]. These factors notably increase the life-cycle CO_{2eq} intensity, which makes using blue H_2 in the CAES systems less beneficial in terms of carbon intensity (Fig. 7).

To assess the environmental impact of CAES systems, we define direct and indirect emission terms in the methodology section. As illustrated in Fig. 8, the relative contributions of these two categories vary across the different D-CAES scenarios. As mentioned before, direct emissions refer to CO_2 generation during the operation of the CAES system, while indirect emissions are caused by life-cyclic processes such as fuel production and leakage. For example, in options where CAES systems are powered by H_2 (both blue and green), substantial share of the total carbon footprint arises from the indirect emission category. This means that the largest fraction of emissions is not directly attributed to the compression or expansion stages, but rather to hydrogen production and the occurrence of gas leakage (CH_4 and H_2). As, blue H_2 is mainly produced from natural gas, both CH_4 and H_2 leakage occur within the process, significantly increases emission rate from leakage. Consequently, the D-CAES scenario with blue H_2 indicates the highest indirect emission rate in Fig. 8, with approximately 79 % of the total emissions. For the case with green H_2 as the fuel, indirect emissions are

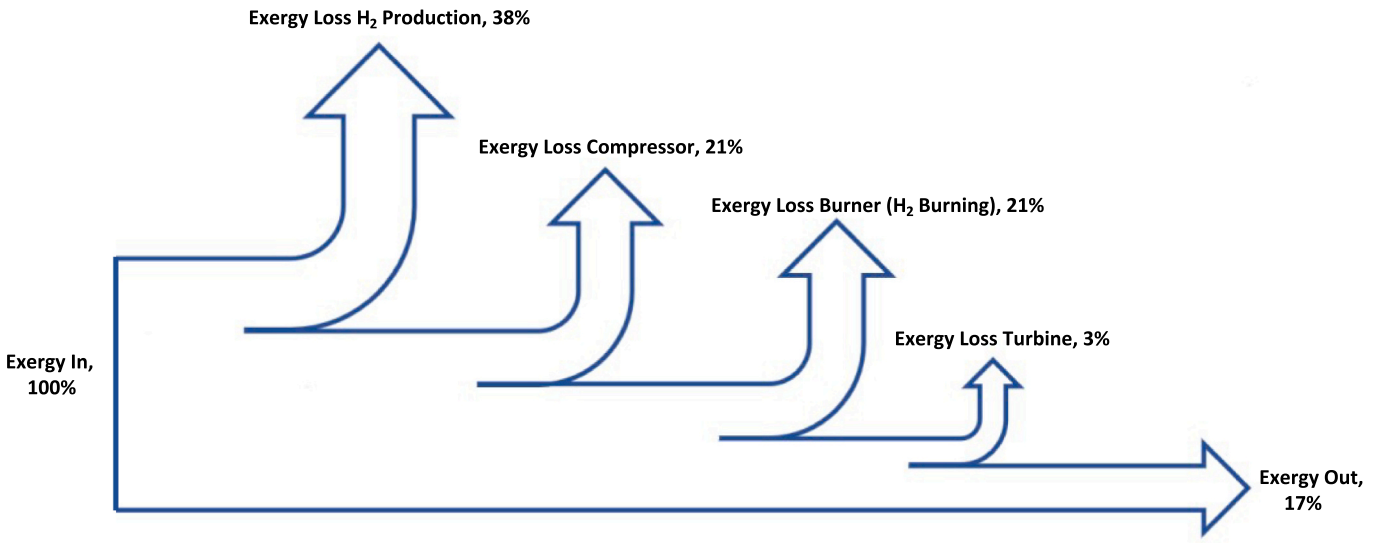

Fig. 6. Exergy flow distribution and average exergy loss fractions for diabatic CAES systems powered by H_2. The results for blue and green H_2 scenarios are similar, therefore they have been averaged into a single representation. (For interpretation of the references to colour in this figure legend, the reader is referred to the web version of this article.)

comparatively lower, around 69 %. Overall, direct emissions account for only 21–31 % of the total emissions in hydrogen-fuelled systems (either blue or green). This includes only the air compression stage. Notably, in these scenarios, there are no carbon emissions from the combustion phase, as combustion of hydrogen does not produce CO_2. Thus, this phase is excluded from the direct emissions category, reducing its overall contribution to the carbon footprint of the system.

In contrast, the CH_4 + CCS configuration exhibits a substantially higher share of direct emissions (90 %), which is largely driven by compression (37 %), combustion (33 %), and CCS operations (20 %). Indirect emissions, such as CH_4 production and leakage, play a comparatively small role, accounting for just 10 % of the total emissions (Fig. 8).

The lowest CO_2 intensity among different CAES configurations is calculated for the A-CAES system. This method eliminates the need for using any additional fuel in the discharging phase leading to reduction in its CO_2 footprint. The total CO_{2eq} intensity of the electricity generation for this system is 12–26 g-CO_{2eq}/MJe with 90–100 % TES efficiency. This involves only the air compression process powered by the low-carbon wind source (Fig. 7).

In summary, the results indicate that, despite utilizing hydrogen as a fuel in the D-CAES system, the life-cycle CO_2 intensity of the system is substantially higher (by an average of 60 %) compared to the A-CAES option. The leakage of methane (in the case of blue hydrogen) and hydrogen during the fuel production and utilization stages significantly exacerbates the total equivalent intensity. Rigorous monitoring and minimization of these leaks could enhance the overall environmental performance of hydrogen-based CAES systems.

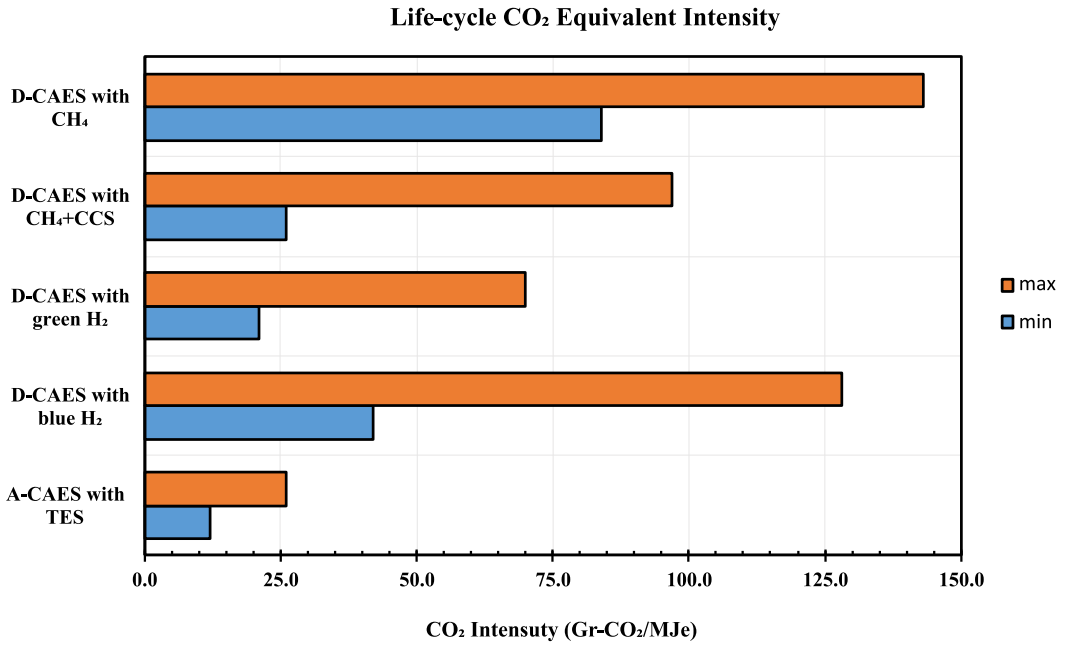

Fig. 7. CO_2 equivalent intensity of different CAES systems.

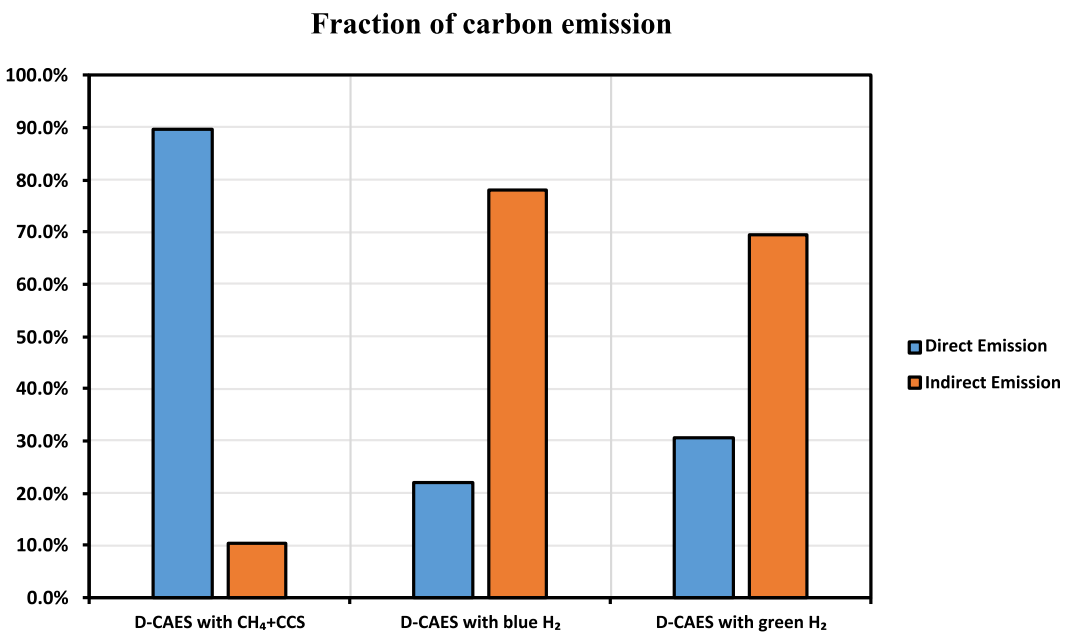

Fig. 8. Average fraction of direct and indirect carbon emissions generated in different diabatic CAES systems.

4.3. Comparison with literature studies

In this section, we compare the results of our exergy analysis with various studies reported in the literature. We selected the most relevant studies for each proposed CAES scenario. The primary distinction of our work is the adoption of a life-cycle approach, as opposed to considering only the operational phase of the system.

For the D-CAES systems powered by natural gas, Elmangart et al. [22] report storage efficiencies ranging from 25 % to 45 %, which closely align with our calculated range of 16 % to 40 %. While their analysis focused solely on the operational phase, our study expands on this by incorporating a life-cycle approach that includes methane production stages. Additionally, they employed a different configuration in the compression stage. These factors primarily account for the slight differences observed. Safei et al. [24] also conducted an exergy analysis of a conventional D-CAES system, reporting an exergy efficiency of 54 %, which does not account for the energy demand of the fuel production stage. Our study further differs in terms of component performance assumptions, utilizing variable ranges for compressor and turbine efficiencies rather than fixed values. This approach allows for a practical evaluation of exergy across a range of operating conditions. Moreover, we consider varying air temperatures at the turbine inlet and outlet and include motor and generator efficiencies, thereby refining our analysis and providing a more comprehensive picture of system performance.

The concept of utilizing hydrogen as fuel in CAES systems is relatively novel, with limited studies available in the literature. Safei et al. [24] investigate the use of hydrogen as fuel in CAES in their study; however, their proposed configuration differs from ours. They utilized the waste heat from compression to produce hydrogen via a high-temperature steam electrolysis process and subsequently used the produced hydrogen as fuel in the turbine. The exergy efficiency of this system is estimated to be 35 %, with fixed values for the inlet and outlet temperatures in the turbine, as well as for the compressor and turbine efficiency.

In contrast, our study considers hydrogen production through various methods, primarily from natural gas and water electrolysis. To capture a realistic range of potential efficiencies, we model variable inlet and outlet temperatures for the turbine air, based on the heat capacity gained from hydrogen combustion. Additionally, we assess the efficiencies of the compressor, turbine, generator, and motor across a range of values, providing a more adaptable model for evaluating maximum and minimum exergy efficiencies under different operational conditions.

Several works have examined the thermodynamic efficiency of A-CAES systems with integrated Thermal Energy Storage (TES). The system proposed for A-CAES by Sciacovelli et al. [21] is similar to our setup, which employs a packed bed for storing the heat generated during the compression stage. They reported a maximum round-trip efficiency between 60 % and 70 %, with TES efficiency above 90 %, closely aligning with our results, where we calculated a maximum exergetic efficiency of 61 %. We also factored in motor and generator efficiencies in this value. Similarly, they found that the greatest exergy losses occurred during the compression stage, while the minimum losses occurred in the TES facility due to heat loss—both outcomes consistent with our findings. In addition, Kim et al. [9] assessed the thermodynamic performance of an A-CAES system with TES, indicating a 68 % electrical storage efficiency, considering the same fixed compressor and turbine efficiency for the system. However, they considered a 50 bar operational pressure for storing air in the cavern, which can result in slight differences in exergy efficiency compared to our study.

5. Conclusion

This study simultaneously evaluates the thermodynamic (exergetic efficiency) and environmental (CO_2 intensity) performance of different Compressed Air Energy Storage (CAES) systems by applying the concept of Exergy-return on Exergy-investment (ERoEI). Various CAES configurations were analysed as potential optimization scenarios. The findings reveal that traditional diabatic CAES system, which powered by CH_4 suffers from significant exergy loss in the charging phase, due to heat dissipation. The thermodynamic efficiency of this system is notably low, which pose a major challenge to its broader adoption and effectiveness. Furthermore, this system also has considerable environmental impact due to high CO_2 emissions associated with CH_4 combustion. The integration of CO_2 capture plants into system reduces the CO_2 intensity in electricity generation, albeit at the expense of reduced exergy efficiency (ERoEI) due to the extra energy demand for CCS plant.

Furthermore, the introduction of hydrogen as a fuel source in the CAES system offers a pathway to achieve higher efficiency due to its higher lower heating value (LHV). The transition to green H_2 as the

primary fuel source for reheating and expansion of air indicates an estimated reduction of 65–76 % in CO_2 intensity. However, it is essential to monitor H_2 and CH_4 leak rates (especially in the case of the use of blue H_2) during the production and utilization of hydrogen, as these leaks can increase remarkably equivalent CO_2 intensity. While the scenario with green H_2 shows a lower CO_2 impact, the overall exergetic efficiency is low due to the high energy cost of producing hydrogen.

The most significant advancement is observed in adiabatic CAES system (A-CAES) with integration Thermal Energy Storage (TES). This system demonstrates the highest exergy efficiency (61 %) and lowest CO_2 intensity (12–26 g-CO_{2eq}/MJe), particularly when full heat recovery is implemented. By capturing the generated heat during air compression stage and retrieve it in discharging phase, this system effectively minimizes additional exergy investment and enhance ERoEI. However, the thermal efficiency of thermal storage facility plays a significant role in this process. If we consider that many TES applications achieve high efficiencies (90–100 %) only over short durations (hours to daily scales), integrating diabatic and adiabatic CAES systems in a hybrid configuration may enhance the capability for longer storage duration.

In conclusion, our life-cycle exergy analysis provides a robust framework balancing the energy demand and environmental challenges in various CAES configurations, offering key insights for system optimization. The results of the exergy analysis combined with future techno-economic considerations, can support stakeholders in identifying the most optimal scenario, with the highest life-cycle efficiency and the lowest environmental impact.

CRediT authorship contribution statement

Boyukagha Baghirov: Writing – original draft, Visualization, Methodology, Investigation, Formal analysis, Conceptualization. **Sahar Hoornahad:** Writing – review & editing, Resources. **Denis Voskov:** Writing – review & editing, Supervision. **Rouhi Farajzadeh:** Writing – review & editing, Supervision, Methodology, Conceptualization.

Author statement

All authors have confirmed their authorship, agreed to the author order as listed, and accept responsibility for their respective contributions to the manuscript.

Declaration of competing interest

The authors declare that they have no known competing financial interests or personal relationships that could have appeared to influence the work reported in this paper.

Acknowledgements

The authors thank Shell Global Solutions International B.V. for granting permission to publish this work. The authors also note that all findings are based on modelled scenarios and literature-derived parameters. The results should be interpreted within the context of the assumptions and analytical scope described in the paper. No commercial or operational guarantees are implied. The views expressed in this publication are those of the authors and do not necessarily reflect the official position or policies of Shell or its affiliates.

Data availability

Data will be made available on request.

7. References

[1] D. Gielen, et al., The role of renewable energy in the global energy transformation, Energ. Strat. Rev. 24 (2019) 38–50.
[2] IEA, Renewables, Available from: *https://www.iea.org/reports/renewables-2023#overview*, 2023.
[3] M. Aneke, M. Wang, Energy storage technologies and real life applications – A state of the art review, Appl. Energy 179 (2016) 350–377.
[4] P.M. Johnson, Assessment of Compressed Air Energy Storage System (CAES), 2014.
[5] Y. Ding, et al., Simulation, energy and exergy analysis of compressed air energy storage integrated with organic Rankine cycle and single effect absorption refrigeration for trigeneration application, Fuel 317 (2022) 123291.
[6] A. EI-Ayoubi, N. Moubayed, Economic study on batteries and hydraulic energy storage for a lebanese hybdrid Wind/PV system, in: 2012 International Conference and Exposition on Electrical and Power Engineering, 2012, pp. 972–977.
[7] H. Yu, S. Engelkemier, E. Gençer, Process improvements and multi-objective optimization of compressed air energy storage (CAES) system, J. Clean. Prod. 335 (2022) 130081.
[8] A.M. Rabi, J. Radulovic, Comprehensive review of compressed air Energy storage (CAES) technologies, Thermo 3 (2023) 104–126, https://doi.org/10.3390/thermo3010008.
[9] Y.-M. Kim, et al., Potential and evolution of compressed air Energy storage: Energy and exergy analyses, Entropy 14 (2012) 1501–1521, https://doi.org/10.3390/e14081501.
[10] M. Jankowski, et al., Status and development perspectives of the compressed air Energy storage (CAES) technologies—A literature review, Energies 17 (9) (2024) 2064.
[11] E. Barbour, et al., Adiabatic compressed air Energy storage with packed bed thermal energy storage, Appl. Energy 155 (2015) 804–815.
[12] H. Jouhara, et al., Latent thermal energy storage technologies and applications: A review, International Journal of Thermofluids 5-6 (2020) 100039.
[13] Q. Zhou, et al., A review of thermal energy storage in compressed air energy storage system, Energy 188 (2019) 115993.
[14] K.J. Khatod, V.P. Katekar, S.S. Deshmukh, An evaluation for the optimal sensible heat storage material for maximizing solar still productivity: A state-of-the-art review, J Energy Storage 50 (2022) 104622.
[15] F. Lei, et al., Thermochemical heat recuperation for compressed air energy storage, Energ. Conver. Manage. 250 (2021) 114889.
[16] L. Szablowski, et al., Energy and exergy analysis of adiabatic compressed air energy storage system, Energy 138 (2017) 12–18.
[17] D. Wolf, M. Budt, LTA-CAES – A low-temperature approach to adiabatic compressed air Energy storage, Appl. Energy 125 (2014) 158–164.
[18] W.F. Pickard, N.J. Hansing, A.Q. Shen, Can large-scale advanced-adiabatic compressed air energy storage be justified economically in an age of sustainable energy? Journal of Renewable and Sustainable Energy 1 (3) (2009).
[19] X. Yu, et al., Evaluation of PCM thermophysical properties on a compressed air energy storage system integrated with packed-bed latent thermal energy storage, J Energy Storage 81 (2024) 110519.
[20] L. Chen, et al., Design and performance evaluation of a novel system integrating water-based carbon capture with adiabatic compressed air energy storage, Energy Convers. Manag. 276 (2023) 116583.
[21] A. Sciacovelli, et al., Dynamic simulation of adiabatic compressed air Energy storage (A-CAES) plant with integrated thermal storage – Link between components performance and plant performance, Appl. Energy 185 (2017) 16–28.
[22] B. Elmegaard, W. Brix, Efficiency of Compressed Air Energy Storage, 2011.
[23] X. Xue, et al., Thermodynamic and economic analysis of new compressed air energy storage system integrated with water electrolysis and H2-fueled solid oxide fuel cell, Energy 263 (2023) 126114.
[24] H. Safaei, M.J. Aziz, Thermodynamic analysis of three compressed air Energy storage systems: Conventional, adiabatic, and hydrogen-fueled, Energies 10 (7) (2017) 1020.
[25] H. Liu, Q. He, S.B. Saeed, Thermodynamic analysis of a compressed air energy storage system through advanced exergetic analysis, Journal of Renewable and Sustainable Energy 8 (3) (2016).
[26] L. Chen, et al., Energy and exergy analysis of two modified adiabatic compressed air energy storage (A-CAES) system for cogeneration of power and cooling on the base of volatile fluid, J Energy Storage 42 (2021) 103009.
[27] M. Rosen, Enhancing Ecological and Environmental Understanding with Exergy: Concepts and Methods. Proceedings of the 4th IASME/WSEAS Int. Conference on Water Resources, 2009.
[28] W. Huang, et al., Exergy-environment assessment for energy system: Distinguish the internal and total exergy loss, and modify the contribution of utility, Energ. Conver. Manage. 251 (2022) 114975.
[29] B. Baghirov, D. Voskov, R. Farajzadeh, Exergetic efficiency and CO2 intensity of hydrogen supply chain including underground storage, Energy Conversion and Management: X 24 (2024) 100695.
[30] R. Farajzadeh, et al., Exergy return on exergy investment and CO2 intensity of the underground biomethanation process, ACS Sustain. Chem. Eng. 10 (31) (2022) 10318–10326.
[31] A.M. Hassan, et al., Exergy return on exergy investment analysis of natural-polymer (guar-Arabic gum) enhanced oil recovery process, Energy 181 (2019) 162–172.
[32] R. Farajzadeh, Sustainable production of hydrocarbon fields guided by full-cycle exergy analysis, J. Pet. Sci. Eng. 181 (2019) 106204.

[33] B. Ghorbani, M. Mehrpooya, A. Ardehali, Energy and exergy analysis of wind farm integrated with compressed air energy storage using multi-stage phase change material, J. Clean. Prod. 259 (2020) 120906.
[34] C. Guo, et al., Comprehensive exergy analysis of the dynamic process of compressed air energy storage system with low-temperature thermal energy storage, Appl. Therm. Eng. 147 (2019) 684–693.
[35] M. Elwardany, A.M. Nassib, H.A. Mohamed, Case Study: Exergy Analysis of a Gas Turbine Cycle Power Plant in Hot Weather Conditions, in: 2023 5th Novel Intelligent and Leading Emerging Sciences Conference (NILES), 2023.
[36] C. Salvini, A. Giovannelli, D. Sabatello, Analysis of diabatic compressed air energy storage systems with artificial reservoir using the levelized cost of storage method, Int. J. Energy Res. 45 (2020) 254–268.
[37] A. Haouam, C. Derbal, H. Mzad, Thermal performance of a gas turbine based on an exergy analysis, E3S Web Conf. 128 (2019) 01027.
[38] National Energy Technology Laboratory, A LITERATURE REVIEW OF HYDROGEN AND NATURAL GAS TURBINES: CURRENT STATE OF THE ART WITH REGARD TO PERFORMANCE AND NOx CONTROL, 2022.
[39] Siemens Energy, Gas turbine portfolio, Available from: https://www.siemens-energy.com/global/en/home/products-services/product-offerings/gas-turbines.html.
[40] R.Z. Aminov, A.B. Moskalenko, A.I. Kozhevnikov, Optimal gas turbine inlet temperature for cyclic operation, J. Phys. Conf. Ser. 1111 (1) (2018) 012046.
[41] Y. Zhang, E. Yao, T. Wang, Comparative analysis of compressed carbon dioxide energy storage system and compressed air energy storage system under low-temperature conditions based on conventional and advanced exergy methods, J Energy Storage 35 (2021) 102274.
[42] B. Baghirov, D. Voskov, R. Farajzadeh, Exergy analysis of adiabatic compressed air energy storage system (A-CAES) 2024 (1) (2024) 1–5.
[43] Yunus A. Çengel, M.A. B., Mehmet Kanoğlu, Chapter 8: Exergy. NINTH EDITION ed., in: THERMODYNAMICS: AN ENGINEERING APPROACH, 2019.
[44] CoolProp Software, Available from: http://www.coolprop.org/.
[45] D.R. Morris, J. Szargut, Standard chemical exergy of some elements and compounds on the planet earth, Energy 11 (8) (1986) 733–755.
[46] H. Mozayeni, X. Wang, M. Negnevitsky, Exergy analysis of a one-stage adiabatic compressed air energy storage system, Energy Procedia 160 (2019) 260–267.
[47] S.S.M. Tan, A. Wahlen, Adiabatic compressed air energy storage: An analysis on the effect of thermal energy storage insulation thermal conductivity on round-trip efficiency, PAM review Energy Science & Technology 6 (2019) 56–72.
[48] A.O. Oni, et al., Comparative assessment of blue hydrogen from steam methane reforming, autothermal reforming, and natural gas decomposition technologies for natural gas-producing regions, Energy Convers. Manag. 254 (2022) 115245.
[49] IEA, Technical Report: Low-Carbon Hydrogen from Natural Gas: Global Roadmap, 2022.
[50] B. Young, et al., Comparative environmental life cycle assessment of carbon capture for petroleum refining, ammonia production, and thermoelectric power generation in the United States, International Journal of Greenhouse Gas Control 91 (2019) 102821.
[51] Y. Tian, et al., Conventional and advanced exergy analysis of large-scale adiabatic compressed air energy storage system, J Energy Storage 57 (2023) 106165.
[52] Ipieca, Compressors, Available from: https://www.ipieca.org/resources/energy-efficiency-solutions/compressors-2022, 2022.
[53] J. Young, US Department of Energy (DOE), Field Demonstration of High-Efficiency Gas Heaters. (2014). Available from: https://www.energy.gov/sites/prod/files/2014/11/f19/gas_heater_demo_report_2.pdf.
[54] Isentropic Efficiency – Turbine/Compressor/Nozzle, Available from: https://www.nuclear-power.com/nuclear-engineering/thermodynamics/thermodynamic-processes/isentropic-process/isentropic-efficiency-turbinecompressornozzle/.
[55] M.R. Islam, Chapter 7 - Field guidelines, in: M.R. Islam (Ed.), Reservoir Development, Gulf Professional Publishing, 2022, pp. 737–843.
[56] T. Fleiter, P. Plötz, Diffusion of Energy-Efficient Technologies, 2013.
[57] Y. Khojasteh Salkuyeh, B.A. Saville, H.L. MacLean, Techno-economic analysis and life cycle assessment of hydrogen production from natural gas using current and emerging technologies, Int. J. Hydrog. Energy 42 (30) (2017) 18894–18909.
[58] A. Hodges, et al., A high-performance capillary-fed electrolysis cell promises more cost-competitive renewable hydrogen, Nat. Commun. 13 (1) (2022) 1304.
[59] J.D. Holladay, et al., An overview of hydrogen production technologies, Catal. Today 139 (4) (2009) 244–260.
[60] WNA, Report Comparison of Lifecycle Greenhouse Gas Emissions of Various Electricity Generation Sources, 2011.
[61] R. Dröge, N.E. Ligterink, W.W.R. Koch, TNO Report: Update of the Netherlands List of Fuels in 2021, 2021.
[62] A. Al-Qahtani, et al., Uncovering the true cost of hydrogen production routes using life cycle monetisation, Appl. Energy 281 (2021) 115958.
[63] Z. Fan, H. Sheerazi, A. Bhardwaj, et al., Hydrogen leakage: a potential risk for the hydrogen economy, COLUMBIA SIPA, Center on Global Energy Policy, 2022.
[64] IPCC Report, Climate Change 2013: The Physical Science Basis, 2013.
[65] N.J. Warwick, et al., Atmospheric composition and climate impacts of a future hydrogen economy, Atmos. Chem. Phys. 23 (20) (2023) 13451–13467.